Nonlinear 3D foot FEA modelling from CT scan medical images

P.J. Antunes & G. R. Dias
IPC – Institute for Polymers and Composites, University of Minho, Guimarães, Portugal
A.T. Coelho
AIS – Amorim Industrial Solutions, Corroios, Portugal
F. Rebelo
Ergonomics Laboratory, Faculty of Human Kinetics, Technical University of Lisbon, Lisbon, Portugal
T. Pereira
The Health Sciences School, University of Minho, Braga, Portugal

ABSTRACT: A 3D anatomically detailed non-linear finite element analysis human foot model is the final result of density segmentation 3D reconstruction techniques applied in Computed Tomography (CT) scan DICOM standard images in conjunction with 3D Computer Aided Design operations and finite element analysis (FEA) modelling. Density segmentation techniques were used to geometrically define the foot bone structure and the encapsulated soft tissues configuration. The monitoring of the contact pressure values at the foot plantar area assumes a vital role on the human comfort optimization. The contact pressure distribution at the plantar area and stresses at the bone structures are calculated for this article for a rigid and direct contact between the plantar foot area and the ground support. Linear and non-linear elastic constitutive material models were implemented to mechanically characterize the behaviour of the biological materials. Furthermore, an experimental validation of the FEA rigid-based contact pressure results is presented.

1 INTRODUCTION

Finite element analysis (FEA) can be a very powerful tool in the foot biomechanical study. The human foot comfort can be related with the contact pressure generated at the plantar/insole(soil) interface.

Large values of contact pressure can generate pain or pathologies due to the obstruction of blood circulation in areas with peak values of pressure. The comfort enhancement at the foot region can be achieved by the application of shoe insoles that must be mechanically optimized to simultaneously support the body weight without foot deviations and act as contact pressure reducers in the precarious plantar zones.

The geometrical complexity of the foot structure implies the use of reverse engineering tools in order to obtain a model that can accurately simulate the biomechanical behaviour of the human foot, namely soft tissues and bone structure.

This article describes the methodology applied in the development of an anatomically detailed three-dimensional foot model for non-linear finite element analysis from medical image data obtained from a CT scan.

2 MODELLING METHODOLOGY

The complex mechanical behaviour of the foot and the necessity of obtaining accurate results for posterior validation with experimental values implies an adequate modelling of the foot structure in terms of 3D anthropometrical characteristics and material constitutive modelling.

The initial step concerning the foot anthropometrical definition was a CT scan of the foot region of a 26 years old male. The DICOM images generated in the CT scan were processed with a medical imaging and editing software (MIMICS® 9.1) that was used to obtain the primary 3D models using density segmentation techniques. The generated primary 3D models were exported as geometrical files for a CAD system (CATIA®) that allowed the assembly and some 3D geometrical operations. Finally, the CAD model was exported to a non-linear FEM/FEA package (ABAQUS® 6.6.1). The model was then prepared for the non-linear structural analysis, namely, through the definition of loads, boundary conditions, material constitutive models, kinematic constraints and finite element mesh generation.

3 MEDICAL IMAGE DATA GENERATION

A CT scan was performed in a 26 years old male, height 175cm and 75kg weight in a Phillips® Brilliance 16 CT scan equipment. The scan was realized for both foot at the neutral posture and was defined by 482 cross-sectional cuts with a slice distance of 0.4mm and a field of view (FOV) of 346mm. The medical images were exported in the DICOM format

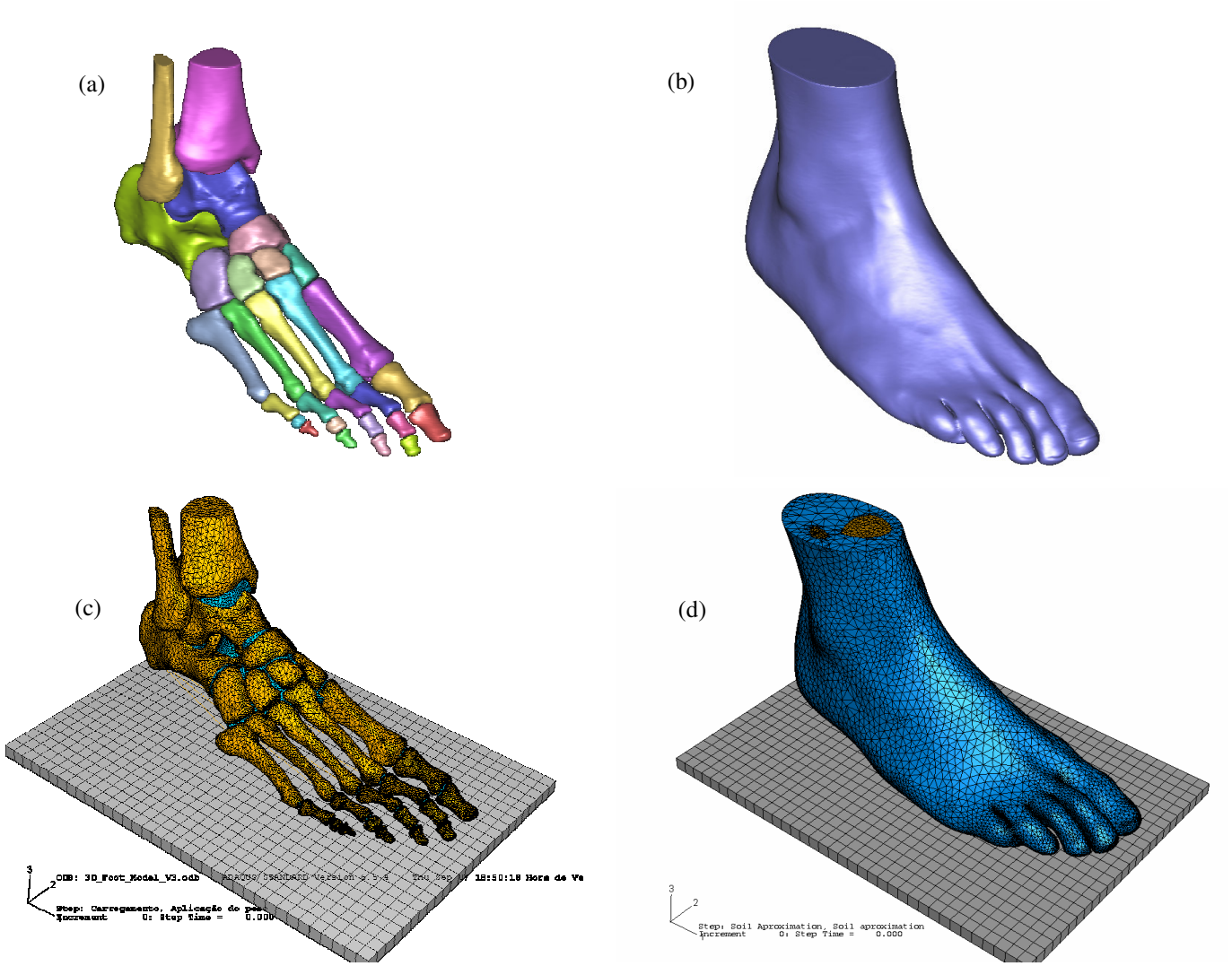

Figure 1. (a) Bone structure segmented model, (b) Soft tissues segmented model, (c) Bone structure FEA model, (d) Bone structure + soft tissues FEA model

with an image area of 1024x1024 pixels. The high image resolution associated with the reduced distance between slices assures a good geometrical definition of the primary 3D models in the future density segmentation operations.

4 3D MODELLING

4.1 *3D reconstruction (density segmentation)*

For the reconstruction of the primary 3D anthropometrical models (bone structure and encapsulated soft tissues) was used the MIMICS® 9.1 medical imaging density segmentation software. Thresholding based on Hounsfield units was used to separate each bone from the bone structure (Fig. 1a) and also for the definition of the encapsulated soft tissues volume (Fig. 1b). In order to include all the cortical and trabecular bone at the foot bone structure and exclude the cartilage regions, a lower limit of 250HU and an upper limit of 2000HU were defined. The soft tissues region was generated accounting a lower limit of -200HU and an upper limit of 3071HU.

4.2 *CAD modelling*

The cartilages that were not reconstructed in the segmentation process were then modelled in order to connect the bones and fill the cartilaginous space. After the cartilage modelling process, volume boolean operations were performed to achieve a volume of soft tissues that corresponds to the subtraction of the bone structure coupled with the cartilages. This approach, guarantees the perfect alignment of the models exterior surfaces, what is an important condition for the future finite element model generation.

4.3 *FEA modelling*

The FEA software package ABAQUS® 6.6.1 was used to define the foot FEA bone structure as shown in Figure 1c, consisted of 29 bone parts and cartilaginous regions, that includes all the *distal, medial and proximal phallanges*, 3 *cuneiforms*, *talus*, *calcaneus*, *cuboid*, *navicular*, *tibia* and *fibula* bones. As shown in Figure 1d, the soft tissues region was also defined and involves the bone structure.

Table 1. Material properties and finite element topology/formulation

	Element				
Components	Topology	Formulation	Young's modulus (MPa)	ν	Cross-sectional area (mm^2)
Bone structure	3D-Tetrahedra	Linear	7300	0.3	-
Cartilage	3D-Tetrahedra	Linear	10	0.4	-
Soft tissues	3D-Tetrahedra	Linear, Hybrid	Hyperelastic	≈ 0.5	-
Achilles tendon	1D	Axial Connector element	∞	-	-
Plantar fascia	1D	Truss element (No compression)	350	-	58.6
Soil	Quadrilateral	Rigid element	∞	-	-

The bone and cartilage structure were bonded together forming a unique structure with different material regions as shown in Figure 1c. This structure was then bonded to the soft tissues volume, through the definition of mesh tie kinematic constrains as can be seen in Figure 1d.

The foot/ground interface was defined through contact surfaces, what allow the load transmission between support and foot model and consecutively the generation of a contact pressure field at the foot plantar area. A small-sliding tracking approach associated with a surface to surface contact formulation was defined to model the interaction tangential behaviour. An augmented lagrangian constraint enforcement method was implemented in the definition of the interaction normal behaviour. The friction coefficient between the foot and soil was set to 0.6, using the Coulomb friction model (Zhang et. al 1999).

For the present case, two different types of loading were considered. The first case, consider a pure vertical compression load of the foot defined only by a vertical force (375N) applied in the ground reference point. The second loading case considers simultaneously the force applied in the calcaneus bone through the Achilles tendon and the ground reaction force, in order to simulate the balanced standing. The plantar fascia and Achilles tendon were included in the FEA model through the definition of truss and axial connectors elements respectively.

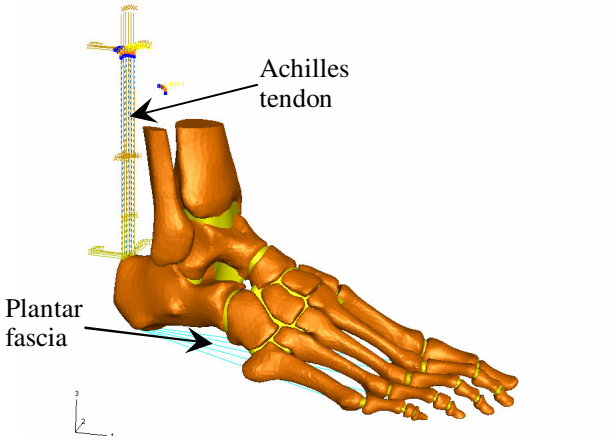

Figure 2. Plantar fascia and Achilles tendon FEA modelling

The plantar fascia is one of the major stabilization structures of the longitudinal arch of the human foot and sustains high tensions during the weight application (Cheung et. al 2004). In the FEA model the plantar fascia was geometrically simplified and divided into 5 separated sections (rays) modelled with truss elements that only supports tensile stress.

The geometrical definition of the Achilles tendon through axial connector elements, allows the simulation of the load applied in the *calcaneus* zone for a foot during balanced standing. The load at the posterior aspect of the *calcaneus* bone is generated by the involuntary contraction of the triceps *surae* muscle group in order to stabilize the foot during standing (Gefen 2002). The study of Simkin (1982), who calculated that the Achilles tendon force should be approximately 50% of the body load during balanced standing, was considered for the present foot computational model.

The upper surfaces of the soft tissues, *tibia* and *fibula* were fixed through the analysis time via a kinematic constraint, while the boundary conditions applied at the soil reference point load, allowed uniquely the plate movement in the vertical (upper) direction.

A wide variety of continuum finite elements topology and formulations were used to descritize the foot model 3D structure. The foot geometrical complexity do not allows the use of hexahedral elements that usually provides higher accuracy with less computational cost.

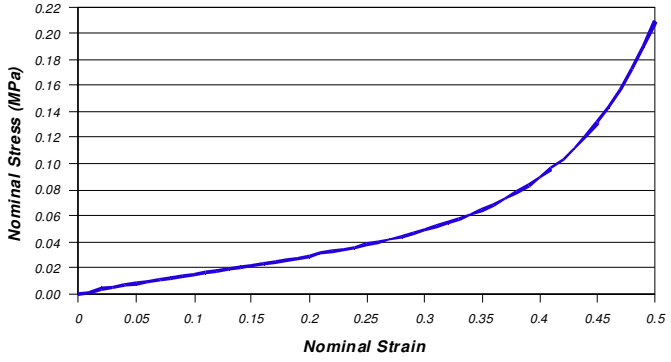

Figure 3. Soft tissues non-linear uniaxial mechanical behaviour

Table 2 Soft tissues hyperelastic material parameters

C_{10}	C_{01}	C_{20}	C_{11}	C_{02}	D_1	D_2
0.08556	-0.05841	0.03900	-0.02319	0.00851	3.65273	0

Table 3 – Contact pressure distribution

Load Case	1st Metatarsal	2nd Metatarsal	3rd Metatarsal	4th Metatarsal	5th Metatarsal	Calcaneus
Pure compression	0.073 MPa	0.042 MPa	0.073 MPa	0.074 MPa	0.018 MPa	0.131 MPa
Balanced Standing	0.083 MPa	0.051 MPa	0.084 MPa	0.083 MPa	0.041 MPa	0.111 MPa

Tetrahedral elements that are more versatile to capture the irregularly shapes of the bone structure and the encapsulated soft tissues, were used to mesh the model. Hybrid element formulation was used to assure the almost-incompressible constraint for the soft tissues non-linear elastic mechanical behaviour. Rigid elements were implemented to define the ground support.

All the materials (Table 1) were considered isotropic and linear-elastic except the soft tissues that are mechanically characterized by a non-linear elastic behaviour. The bone material behaviour was linearly defined with a Young's Modulus and Poisson's ratio (ν), equal to 7300 MPa and 0.3, respectively. These values were obtained by weighing cortical and trabecular bone elasticity according to Nakamura et al. (1981). The mechanical properties of the cartilage (Shanti et. al 1999 & Gefen 2003) and plantar fascia (Cheung et. al 2005), were selected from the literature. Specifically, the bulk soft tissues non-linear elastic mechanical behaviour definition was based on the uniaxial stress-strain data obtained from *in vivo* tests of the heel (Lemmon et al. 1997). The bulk soft tissues non-linear mechanical behaviour was defined through a hyperelastic model based on a second order polynomial strain energy function (Cheung et. al 2005 & Lemmon et al. 1997), given by the expansion of Equation.1.

$$\psi\left(J,\bar{I}_1,\bar{I}_2\right)=\sum_{i+j}^{N} C_{ij}\left(\bar{I}_1-3\right)^i\left(\bar{I}_2-3\right)^j+\psi_{vol}\left(J\right) \quad (1)$$

Setting $N=2$ and considering that the pure volumetric response is given by the strictly convex function, given by Equation. 2.

$$\psi_{vol}(J)=\frac{1}{D_i}\left(J-1\right)^{2i} \quad (2)$$

where ψ is the overall strain energy per unit of reference volume; J is the volume ratio; C_{ij} and D_i are material dependent parameters obtained from the experimental data; $\bar{I}_1$ and $\bar{I}_2$ are the modified strain invariants. The material parameters used for the definition of the hyperelastic model associated with the non-linear mechanical definition of the soft tissues, are presented in Table 2.

5 NON-LINEAR FEA RESULTS

The anatomically detailed 3D FEA foot model was developed from CT scan images using density segmentation techniques and CAD manipulation. Kinematic constrains between bone structures, cartilages and soft tissues were defined. The load transmission between ground support and the foot structure was defined by the introduction of contact pairs, namely, at the foot plantar area/ground support interface.

Large deformations and non-linear geometrical analysis associated with material nonlinearities were considered.

The created FEA model allows the output of several results that can be used for comfort evaluation of shoe insoles or to study other biomechanical aspects of the foot. The monitoring of contact pressure values at the foot plantar area assumes a vital role on this study. The results were obtained considering two different load cases, namely, pure compression load (weight load) and balanced standing load (weight load + Achilles tendon load).

The FEA model predicts a maximum plantar contact pressure value of 0.131 MPa (13.1 N/cm^2) and 0.111 MPa (11.1 N/cm^2) for the pure compression (Fig. 5), and balanced standing case respectively, at the heel region.

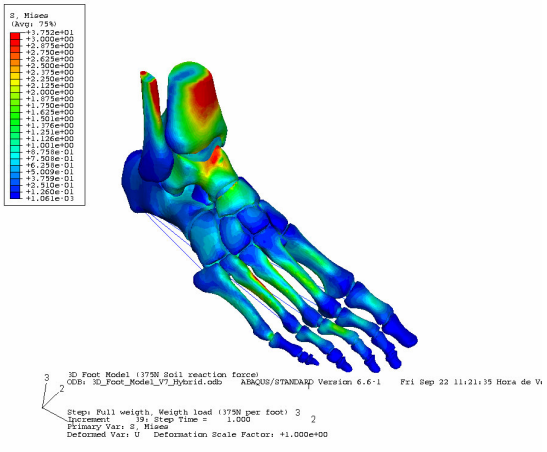

Figure 4. Von Mises stress at the bone structure

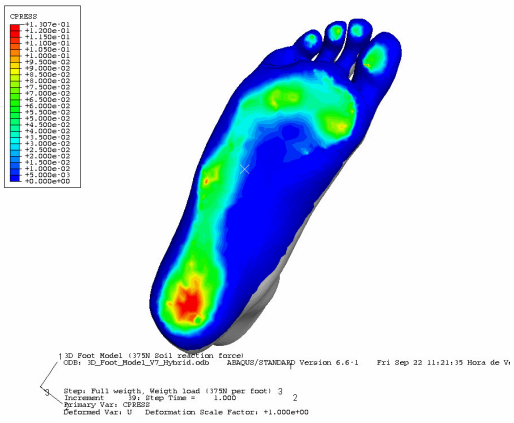

Figure 5. Contact pressure values at the foot plantar are (pure compression)

The contact pressure under the *metatarsal* heads and the *distal phalanges* increases with the load application at the posterior *calcaneus* (through the Achilles tendon). The load at the *calcaneus* compared with the pure compression load, displaces the centre of pressure and increases the load-bearing at the forefoot reducing consequently the load-bearing at the rearfoot. At the bone structure, peak of stress are present at the *metatarsal* and *talus* bones (Fig. 4). The insertion points of the fascia plantar truss elements at the *phalanges/metatarsal* connection region and *calcaneus* bone, experienced large stress due to the generated fascia plantar tension. In Table 3 are presented indicative nodal contact pressure values at the same nodes beneath the *metatarsal* heads and heel regions. The FEA predicted centre of pressure for the balanced standing model was approximately located at the 2nd cuneiform.

6 EXPERIMENTAL VALIDATION

6.1 *Methodology*

For a quantitative evaluation of the contact pressure generated at the plantar foot area, the same individual that volunteered for the CT scan was used to experimentally evaluate the pressure distribution during barefoot balanced standing. For this experimental study a podologic pressure measuring equipment from Eclipse 2000® was used (Fig. 6a).

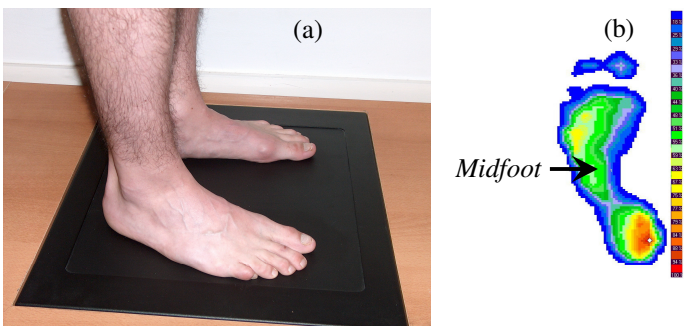

Figure 6. (a) Podologic pressure measuring test, (b) experimental foot plantar contact pressure distribution.

A barefoot balanced standing posturologic test was conducted during 10s, where the contact pressure values were evaluated 200 times in that time range, corresponding to a results output frequency of 20Hz. The mean contact pressure value was automatically calculated by the equipment software. In Figure 6b is showed the experimental contact pressure values distribution for the right barefoot balanced standing situation.

6.2 *Comparison of experimental and FEA results*

The obtained experimental results were compared with the FEA results obtained for the balanced standing case. An experimental peak pressure for the foot plantar area of about 0.071MPa (7.1N/cm^2) is measured at the heel region. The FEA model predicts a maximum value for the same area but greater and equal to 0.111MPa (11.1N/cm^2). In a midfoot indicative point as displayed in Figure 6b, the experimental contact pressure is approximately equal to 0.038MPa (3.8N/cm^2), while the correspondent FEA predicted pressure for approximately the same point is equal to 0.049MPa (4.9N/cm^2). Beneath the *metatarsal* heads, indicative experimental contact pressure values of about 0.033, 0.039, 0.045, 0.387 and 0.045MPa from the 1st to 5th *metatarsal* head were measured, while the correspondent FEA nodal contact pressure values were about the following ranges: [0.053, 0.103], [0.041, 0.051], [0.051, 0.088], [0.039, 0.098] and [0.041, 0.067]MPa, for approximately the same foot regions. Notice that the FEA values are taken in a min/max form due to the difficulty in obtaining a single contact pressure value for those zones. The FEA predicted contact area was approximately equal to 89cm^2, compared to 138cm^2 obtained from the experimental measurements.

7 DISCUSSION

The FEA capability in predicting the stress state in the foot, namely the contact pressure at the foot plantar area, makes suitable the application of the present model in the comfort optimization of shoe insoles or other foot support devices. This model describes the geometry of the ankle-foot complex and contains information about the bony, cartilaginous, plantar fascia and soft tissues materials mechanical behaviour. The experimental plantar contact pressure distribution is qualitatively comparable with the predicted FEA results, nominally, the peak pressure values zones at the centre of the heel region and beneath the *metatarsal* heads. However in the quantitative point of view the FEA results are higher than the experimental results. This difference may be caused by the resolution of the pressure sensors that report an average pressure over a sensor area while the FEA model reports the contact pressure as calculated

from a nodal force per element's surface area. Therefore is expected that the FEA contact pressure results be higher than the experimental ones. The predicted FEA results showed that at the heel region and beneath the *metatarsal* heads the contact pressure values were maximum what indicate the regions that most probably ignite foot pain and ulcer development. These results are in accordance with the observation of foot ulcers appearance at the medial forefoot and heel regions of the diabetic patients (Mueller et. al 1994 & Raspovic et. al 2000).These regions must be protected with deformable insole materials that accommodates deformation and reduce the contact pressure trough the local increase of the contact area.

The FEA predicted contact area values for balanced standing ($89cm^2$) are proportionally comparable with the results obtained by Cheung et. al (2005), who reported a contact area equal to $68cm^2$ for a 1.74m and 70kg male with normal soft tissues stiffness. The higher contact area values obtained in our experimental results can be due to the contact area acquisition mode and sensors resolution at the podologic pressure measuring equipment.

The centre of pressure predicted with the FEA model is approximately in accordance with the results obtained by Simkin (1982) who reported a centre of pressure located at the 3^{rd} cuneiform or for some cases, between the 2^{nd} and 3^{rd} cuneiform.

The difficulty in obtaining a completely static posture that replicates the FEA model load condition was a major experimental difficulty encountered and an aspect that must be accounted during the results evaluation and discussion. In fact, the continuous individual displacement originated by the involuntary muscle contraction during balanced standing can affect the foot load bearing and consequently the experimental contact pressure distribution and its values.

8 CONCLUSIONS AND FUTURE WORK

The finite elements method can be a very powerful method to understand the foot mechanical behaviour and its implications to human foot comfort. The present non-linear FEA model intends to be a tool for the design optimization process of shoe insoles. For that purpose, an anatomically detailed foot model was generated from CT scan image data using segmentation reconstruction techniques and 3D CAD modelling operations.

In the present model, several material constitutive models were considered. Kinematic constraints and parts interactions, namely, at the foot plantar/soil interaction were implemented. Achilles tendon and plantar fascia were introduced considering some geometrical simplifications.

The FEA contact pressure values were experimentally verified by the use of a podologic pressure measuring equipment. The effect of the load application at the Achilles tendon was also studied to understand its effect on the contact pressure distribution at the foot plantar area.

A wide variety of insole geometries and materials can in the future be tested in order to study and improve the foot comfort through the modification of insole geometrical design and/or insole materials formulation.

The introduction of the foot ligament and muscular structure is predicted to be incorporated in future FEA works to dynamically model the human gait.

9 REFERENCES

Camacho, D.L.A. & Ledoux, W.R. & Rohr, Eric S. & Sangeorzan, B.J. & Ching, Randal P. 2002. A Three-Dimensional, anatomically detailed Foot Model: A Foundation for a Finite Element Simulation and Means of Quantifying Foot-Bone Position; *Journal of Rehabilitation Research & Development* 39:401:410.

Cheung, J.T & Zhang, M & Leung, A.K.L. & Fan, Y.B. 2005. Three Dimensional Analysis of the Foot During Standing – A Material Sensitivity Study; *Journal of Biomechanics* 38: 1045-1054.

Cheung, J.T. & Zhang, M. & An, K.N. 2006. Effect of Achilles Tendon Loading on Plantar Fascia Tension in the Standing Foot. *Clinical Biomechanics* 21:194-203.

Cheung, J.T. & Zhang, M. & An, K.N. 2004. Effects of Plantar Fascia Stiffness on the Biomechanical Responses of the Ankle-Foot Complex. *Clinical Biomechanics* 19:839-846.

Gefen, A. 2003. Plantar Soft Tissue Loading Under the Medial Metatarsals in the Standing Diabetic Foot. *Medical Engineering & Physics* 25: 491-499.

Gefen, A. 2002. Stress Analysis of the Standing Foot Following Surgical Plantar Fascia Release. *Journal of Biomechanics* 35: 629-637.

Lemmon, D. & Shiang, T.Y. & Hashmi, A. & Ulbrecht, J.S. & Cavanagh, P.R. 1997. The Effect of Shoe Insoles in Therapeutic Footwear – A Finite Element Approach. *Journal of Biomechanics* 30:615-620.

Mueller, M.J. & Sinacore, D.R. & Hoogstrate, S. & Daly, L. 1994. Hip and ankle walking strategies:effect on peak plantar pressures and implications for neuropathic ulceration. *Archives of Physical Medicine and Rehabilitation* 75: 1196-1200.

Nakamura S. & Crowninshield R.D. & Cooper R.R. 1981. An Analysis of Soft Tissue Loading in the Foot: a preliminary report. *Bulletin of Prosthetics Research* 18:27-34

Raspovic, A. & Newcombe, L. & Lloyd, J. & Dalton, E. 2000. Effect of customized insoles on vertical plantar pressures in sites of previous neuropathic ulcerations in the diabetic foot. *The Foot* 10: 133-138.

Shanti, J. & Mothiram K. P. 1999. Three Dimensional Foot Modelling and Analysis of Stresses in Normal and Early Stage Hansen's Disease with Muscle Paralysis *Journal of Rehabilitation Research & Development* 36.

Simkin, A. 1982. Structural Analysis of the Human Foot in-Standing Posture. PhD Thesis, Tel Aviv University.

Zhang, M & Mak, A.F.T. 1999. In vivo skin frictional properties. *Prosthetics and Orthotics International* 23: 451-456.